Version 1 CONF-970713--3

March 24, 1997

Random-field critical scattering at high magnetic concentration in the Ising antiferromagnet $Fe_{0.93}Zn_{0.07}F_2$

Z. Slanič [a], D.P. Belanger [a] and J.A. Fernandez-Baca [b]

[a] Department of Physics, University of California, Santa Cruz, CA 95064 USA

[b] Solid State Division, Oak Ridge National Laboratory, Oak Ridge, TN 37831-6393 USA

Abstract

The high magnetic concentration Ising antiferromagnet $Fe_{0.93}Zn_{0.07}F_2$ does not exhibit the severe critical scattering hysteresis at low temperatures observed in all lower concentration samples studied. The system therefore provides equilibrium neutron scattering line shapes suitable for determining random-field Ising model critical behavior.

Keywords: Critical phenomena, Dilute antiferromagnet, Neutron scattering - critical, Random fields

David P. Belanger, Department of Physics, University of California, Santa Cruz, CA 95064, USA

FAX: (805)459-3043

email: dave@dave.ucsc.edu

It is well known that a phase transition occurs[1] for the $d = 3$ random-field Ising model (RFIM). However, critical behavior investigations using the experimental realizations, anisotropic randomly dilute antiferromagnets such as $Fe_xZn_{1-x}F_2$ in applied uniform fields, have been very challenging, primarily as a result of severe hysteresis in scattering line shapes below the transition $T_c(H)$. This is most evident when comparing data taken upon cooling in a field (FC) and heating in the field after cooling in zero field (ZFC). It has been shown[2, 3] that, at large dilution, the system breaks into weakly interacting domains as $T \rightarrow T_c(H)$ after ZFC to establish long-range order. For $x < 0.8$, vacancies are so numerous that domain walls form with little energy cost. This effect obscures the decrease of the order parameter within domains due to thermal fluctuations since the Bragg intensity vanishes with domain formation. In the present study, we have overcome this problem by employing a magnetically concentrated crystal, $Fe_{0.93}Zn_{0.07}F_2$, in which domains cannot form without the energy penalty of breaking many magnetic bonds, as in the original ferromagnetic RFIM.

The scattering measurements were made at the Oak Ridge National Laboratory High Flux Reactor using a two-axis spectrometer configuration. We used the (0 0 2) reflection of pyrolytic graphite (PG) at an energy of 14.7 meV to monochromate the beam. We employed three different collimation configurations. The lowest resolution is with 70 min of arc before the monochromator, 40 before the sample and 40 after the sample. We also took scans with 20 min of arc before and after the sample and with 10 min of arc before and after the sample. PG filters were used to eliminate higher-order scattering. The carbon thermometry scale was calibrated to agree with recent specific heat results[4] for the $H = 0$ transition. The field dependence of the thermometry was also calibrated and $T_c(H) - T_c(0)$ is consistent with the

DISCLAIMER

Portions of this document may be illegible in electronic image products. Images are produced from the best available original document.

specific heat data. The rounding of the transition occurs only for $|t| < 2 \times 10^{-3}$, allowing the critical behavior to be probed reasonably well.

Four transverse ZFC scans across the antiferromagnetic (1 0 0) Bragg point with fine collimation are shown in Fig. 1. Two scans are at 0.13 and 0.31 K above $T_c(H) = 70.62K$ and the others are 0.14 and 0.20 K below. The contrast between the scans above and below $T_c(H)$ is striking. All scans taken at $H = 0$ and those below $T_c(H)$ for $H > 0$ can be reasonably fit to the mean-field Lorentzian line shape

$$S(q) = \frac{A}{q^2 + \kappa^2} + {M_s}^2\delta(q) \quad , \tag{1}$$

where $\kappa(T)$ is the inverse correlation length for fluctuations and M_s is the staggered magnetization. The mean-field RFIM prediction includes a squared Lorentzian term

$$S(q) = \frac{A}{q^2 + \kappa^2} + \frac{B}{(q^2 + \kappa^2)^2} + {M_s}^2\delta(q) \quad , \tag{2}$$

but the $H > 0$ and $T < T_c(H)$ fits allow no significant contribution from this term. Above $T_c(H)$ Eq. 1 does not fit the data well and Eq. 2 is more appropriate. The fitted behavior for the staggered susceptibility, $\chi(T)$, and $\kappa(T)$, obtained from the Lorentzian term, do not behave consistently as explained below. We therefore emphasize that these equations are not adequate, perhaps because the RFIM exponent η, a measure of the deviation from mean-field behavior, is quite large[1].

The $q = 0$ Bragg intensity is very large just below $T_c(H)$ and vanishes just above, in accordance with Monte Carlo results[5] that β is close to zero. The small hysteresis observed in the Bragg intensity upon FC and ZFC is consistent with the extinction effects.

The $|q| > 0$ line shapes also show a dramatic change at $T_c(H)$ with no hysteresis. For the previous studies at $x = 0.52$[2] and 0.46[3], the $|q| > 0$ intensities grow much more rapidly as $T \to T_c(H)$ and, concomitantly, the Bragg scattering exhibits an anomalous decrease in intensity, effects attributed[2] to domain formation which are apparently absent for $x = 0.93$.

$\kappa(T)$ and $\chi(T)$ are shown in Fig. 2 and Fig. 3, respectively, for both $H = 0$ and $H = 7T$. In both cases $\kappa(T)$ decreases to approximately the resolution limit of 2×10^{-3} reciprocal lattice units. At $H = 0$, the values of $\kappa(T)$ and $\chi(T)$ fit well to random-exchange behavior[6] above and below $T_c(H)$, with $\nu = 0.71 \pm 0.01$ and $\gamma = 1.35 \pm 0.01$, respectively. For $H = 7$ T, the values $\nu = 0.90 \pm 0.01$ and $\gamma = 1.72 \pm 0.02$ for $T > T_c(H)$ are consistent with earlier experiments[7], simulations[5] and theory[8]. The disconnected staggered susceptibility exponent $\bar{\gamma} = 3.0 \pm 0.1$ is also in reasonable agreement with previous results[7]. However, the values of $\kappa(T)$ and $\chi(T)$ for $T < T_c(H)$ are inconsistent with any power laws and fits are consequently not shown. The results for $\kappa(T)$ and $\chi(T)$ for $T < T_c(H)$ are very dependent on the scattering line shapes used in the analysis and further discussion will be deferred to a more extensive report. The values for $\kappa(T)$ and $\chi(T)$ are independent of the cooling procedure, implying equilibrium behavior.

We have demonstrated in this report that the equilibrium critical behavior of RFIM dilute antiferromagnets is accessible to experiments if the magnetic concentration is sufficiently high. We observe no hysteresis for $|q| > 0$ well below $T_c(H)$, unlike the case of $x < 0.8$.

This work has been supported by DOE Grant No. DE-FG03-87ER45324 and by ORNL, which is managed by Lockheed Martin Energy Research Corp. for the U.S. DOE under contract number DE-AC05-96OR22464.

References

[1] For a review, see D.P. Belanger and A.P. Young, J. Mag. Mag. Mater. 100 (1991) 272.

[2] D.P. Belanger, J. Wang, Z. Slanič, S.-J. Han, R.M. Nicklow, M. Lui, C.A. Ramos, and D. Lederman, J. Magn. Magn. Mater. 140-144 (1995) 1549; Phys. Rev. B 54 (1995) 3420.

[3] D.P. Belanger, A.R. King, V. Jaccarino, and R.M. Nicklow, Phys. Rev. Lett. 59 (1987) 930.

[4] Z. Slanič and D.P. Belanger, submitted for publication, 1997.

[5] H. Rieger, Phys. Rev. B 52 (1995) 6659.

[6] D.P. Belanger, A.R. King and V. Jaccarino, Phys. Rev. B 34 (1986) 452.

[7] D.P. Belanger, A.R. King and V. Jaccarino, Phys. Rev. B 31 (1985) 4538.

[8] M. Gofman, J. Adler, A. Aharony, A.B. Harris and M. Schwartz, Phys. Rev. B 53 (1996) 6362.

Figures:

Fig. 1. The logarithm of the neutron scattering intensity vs. q just above and below $T_c(H)$.

Fig. 2. The inverse correlation length κ vs. T for $H = 0$ and 7 T.

Fig. 3. The logarithm of the staggered susceptibility χ vs. T for $H = 0$ and 7 T.

Figure 1 - Z. Slanič

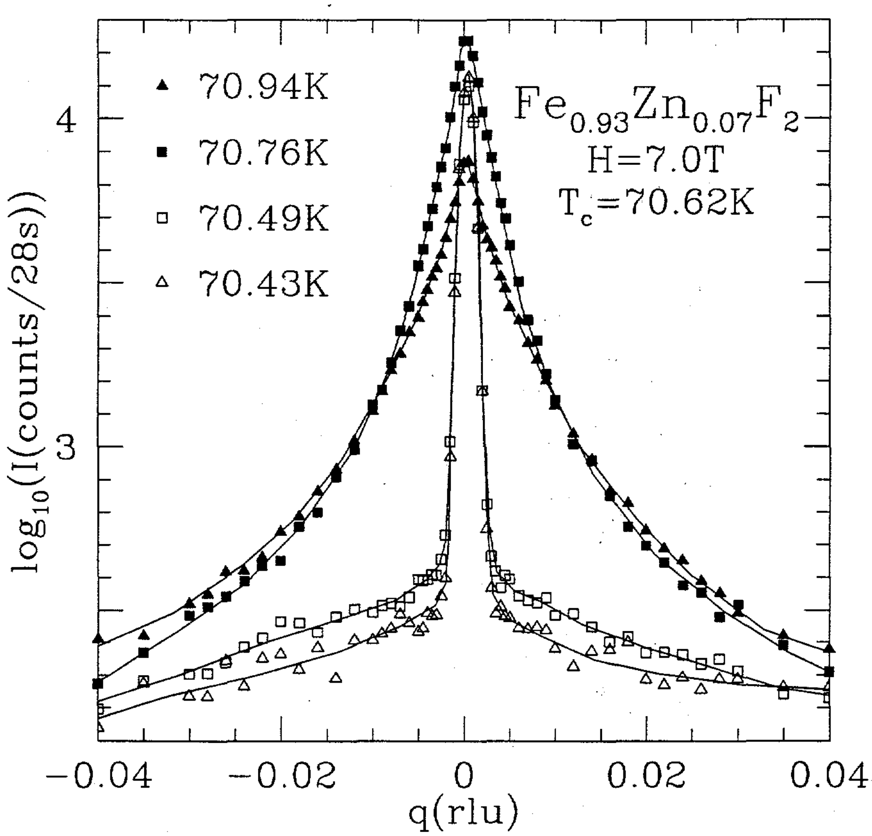

Figure 2 - Z. Slanič

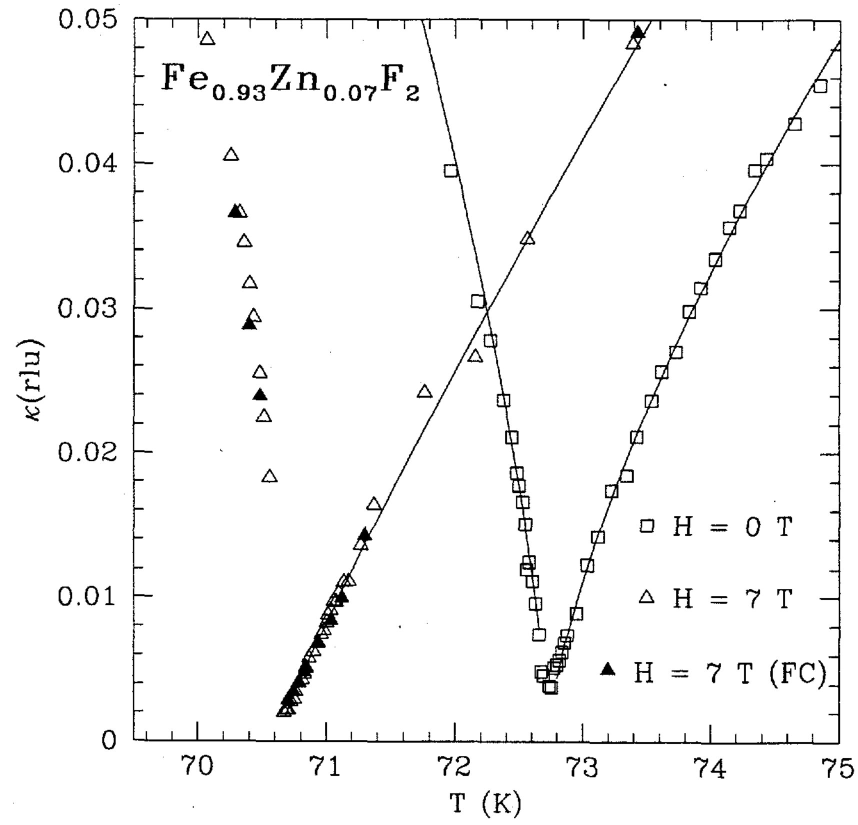

Figure 3 - Z. Slanič

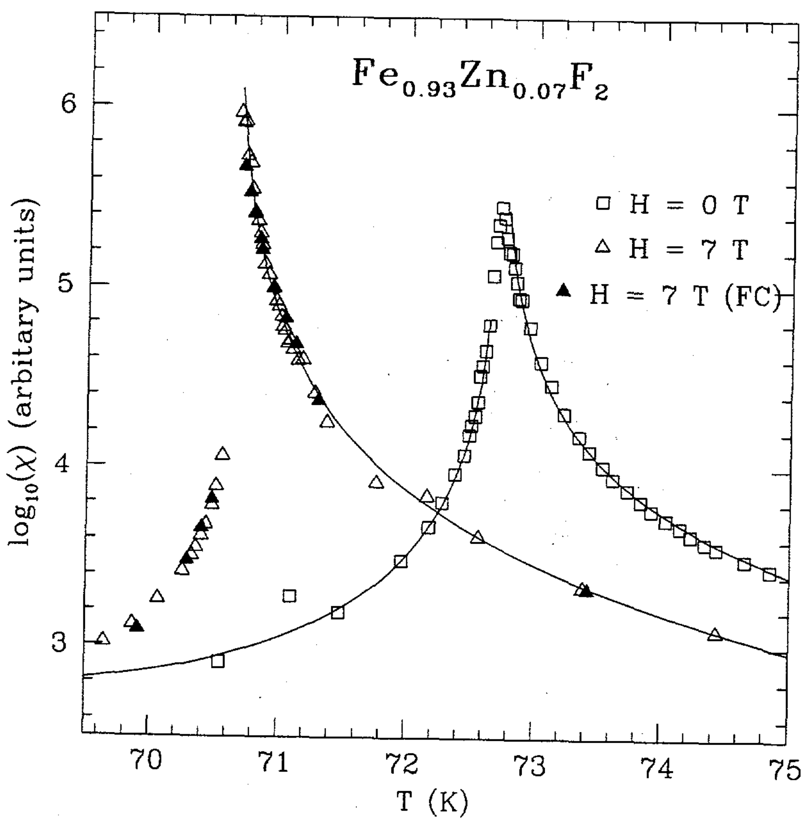

DISCLAIMER

This report was prepared as an account of work sponsored by an agency of the United States Government. Neither the United States Government nor any agency thereof, nor any of their employees, makes any warranty, express or implied, or assumes any legal liability or responsibility for the accuracy, completeness, or usefulness of any information, apparatus, product, or process disclosed, or represents that its use would not infringe privately owned rights. Reference herein to any specific commercial product, process, or service by trade name, trademark, manufacturer, or otherwise does not necessarily constitute or imply its endorsement, recommendation, or favoring by the United States Government or any agency thereof. The views and opinions of authors expressed herein do not necessarily state or reflect those of the United States Government or any agency thereof.